RSC Advances

REVIEW

View Article Online
View Journal | View Issue

Cite this: *RSC Adv.*, 2021, **11**, 5411

Recent developments in voltammetric and amperometric sensors for cysteine detection

Somayeh Tajik,[a] Zahra Dourandish,[b] Peyman Mohammadzadeh Jahani,[c] Iran Sheikhshoaie,[b] Hadi Beitollahi,*[d] Mehdi Shahedi Asl,[e] Ho Won Jang*[f] and Mohammadreza Shokouhimehr*[f]

Received 5th September 2020
Accepted 6th December 2020

DOI: 10.1039/d0ra07614g

rsc.li/rsc-advances

This review article aims to provide an overview of the recent advances in the voltammetric and amperometric sensing of cysteine (Cys). The introduction summarizes the important role of Cys as an essential amino acid, techniques for its sensing, and the utilization of electrochemical methods and chemically modified electrodes for its determination. The main section covers voltammetric and amperometric sensing of Cys based on glassy carbon electrodes, screen printed electrodes, and carbon paste electrodes, modified with various electrocatalytic materials. The conclusion section discusses the current challenges of Cys determination and the future perspectives.

Introduction

The human body contains a lot of biomolecules, such as proteins, nucleic acids, amino acids, carbohydrates and so on, which dominate the physiological functions of the body. However, abnormal concentrations of the biomolecules can cause multiple illnesses. Hence, it is very important to selectively and sensitively detect biomolecules for pharmaceutical preparations and clinical diagnosis. Amino acids are generally considered to be molecules consisting of a carboxylic acid group, a side-chain, and an amine group, which are specific to each amino acid. The major elements of amino acids have been found to be hydrogen, carbon, nitrogen and oxygen.[1] In addition, it is possible to use amino acids as the building blocks of proteins, which are linear chains of amino acids. In addition, amino acids may be associated together in different sequences for forming diverse proteins.

Cys, which has been proposed to be a small molecule consisting of sulfur, contributes to fundamentally important biological processes[2,3] such as regulating the function and structure of proteins *via* reactive thiols, triggering the synthesis of glutathione for the improvement of embryo generation.[4,5] Moreover, the body transforms Cys into glucose as one of the sources of energy and plays a significant part in communicating between the immune system cells. Furthermore, Cys is reported to contribute critically to the conformation and assembly of receptors.[6] The usual concentration of Cys in the blood plasma is between 53 and 300 mM and it can be utilized as a prominent indicator of health conditions and risk of disease.[7] In addition, Cys deficiency results in slower growth of the body, skin lesions, hair de-pigmentation, liver damage, edema, muscle and fat loss, weakness and lethargy.[8–10] Consequently, abnormal accumulation and formation of Cys have been expressed through neurological pathogeneses, cystinosis, Alzheimer's and Parkinson's diseases and metabolic disorders.[11] Hence, designing quick, inexpensive, reliable, as well as sensitive, analytical methods to detect Cys would be of high prominence for quantifying proteins and for earlier diagnosis and prevention of neurological disorders such as Parkinson's and Alzheimer's diseases and motor neuron disease.

Various procedures have been developed to detect Cys, including chromatography,[12] chemiluminescence,[13] spectrofluorimetry,[14] spectrophotometry,[15] and colorimetry.[16] However, some of the aforementioned methods are laborious, expensive, and demand complex preconcentration, multi-solvent extraction and expert personnel. Consequently, it is highly necessary to develop a simple strategy for the detection of Cys. Electrochemical procedures have general advantages such as simplification, high stability and sensitivity, affordable equipment, and on-site supervision.[17,18] Nonetheless, even though L-cysteine is considered to an electro-active molecule, a number of problems have been found in the electroanalysis, such as a larger overpotential, lower sensitivity, as well as inactive electron

[a]*Research Center for Tropical and Infectious Diseases, Kerman University of Medical Sciences, Kerman, Iran*

[b]*Department of Chemistry, Faculty of Science, Shahid Bahonar University of Kerman, Kerman 76175-133, Iran*

[c]*Department of Basic Sciences, School of Medicine, Bam University of Medical Sciences, Bam, Iran*

[d]*Environment Department, Institute of Science and High Technology and Environmental Sciences, Graduate University of Advanced Technology, Kerman, Iran. E-mail: h.beitollahi@yahoo.com*

[e]*Marine Additive Manufacturing Centre of Excellence (MAMCE), University of New Brunswick, Fredericton, NB, E3B 5A1, Canada*

[f]*Department of Materials Science and Engineering, Research Institute of Advanced Materials, Seoul National University, Seoul 08826, Republic of Korea. E-mail: hwjang@snu.ac.kr; mrsh2@snu.ac.k*

transfer kinetics at the conventional electrodes. Such barriers may result in the formation of oxides and fouling of the electrode surface. To overcome the above described barriers, experts in the field have reported multiple attempts, including electrochemical detection *via* modified electrodes.

The working electrode is an essential contributor to the determination procedure and possesses extensive scope for modification through various electrocatalytic substances.[19,20] In recent years, researchers have considered chemically modified electrodes (CMEs) as a result of the respective potent utilizations in different analyses and the relative simplicity of their construction and regeneration.[21–26] The electrode has been modified for a number of conditions, in which it was impossible to conduct analysis with a bare conductive electrode or enhance sensitivity.[27,28] Modifying the conductive substrate can lead to augmented kinetics for electron transfer. In fact, modifying the electrode surface results in a catalytic part and very little changes at the surface, these features specify the sensitivity of the measurements in electroanalytical utilizations.[29–33] In general, the modified surfaces lead to:

Transfer of the physicochemical features of the modifier to the electrodes;

Greater electrocatalytic activities owing to the use of substances with larger surface areas that allow higher sensitivity;

Selectivity toward the analyte owing to the immobilized functional groups and dopants, quick diffusion kinetics in a number of substances and;

Extraction and accumulation of an analyte at the surface of the electrode.

A number of electrochemical procedures have been used to detect Cys. The electrochemical methods used to detect Cys in an aqueous solution have been categorized based on various electrical signals produced in the solution owing to the presence of Cys. In fact, potentiostatic procedures include utilization of potentiostat instruments for controlling the potential between the reference electrodes and counter electrodes to maintain a potent difference between the working and reference electrodes. The resulting current has been gauged and registered for prediction of the concentration of analytes. These tests are known as the controlled potential procedures. These controlled potential procedures have been categorized into diverse groups with regards to the kind of voltage signals applied and the final measured current wave-forms. Therefore, three fundamental sub-categories of potentiostatic procedures include chronocoulometry, voltammetry/polarography and amperometry. Among these methods, voltammetry and amperometry have been widely used for the determination of Cys.

As demonstrated by experts in the field, amperometry is considered to be a section of the controlled potential procedures, in which very small currents were controlled and gauged at a constant potential with the use of a non-mercury working electrode. In general, this method utilizes a potent step signal that should be provided between the working and reference electrodes in the solution consisting of electroactive specimens. The final reduction at the surface of the electrode results in the flow of very large currents that are proportionate to the concentration gradient at the surface of the electrodes. The current is registered as a function of time and thus these tests are known as amperometric procedures. This procedure determines one chosen component from the electrochemically reducible specimens only, owing to the constant potential of the working electrode. Hence, the analytes that should be determined undergo a faradaic reaction at some desirable polarity and the magnitude of potential applied. Nonetheless, because of the lower surface area of the working electrodes, this faradaic reaction is not complete and just a fraction of the analyte reacts.[34]

Studies have shown the widespread utilization of the voltammetric procedures for determining and measuring analytes in diverse matrices. These procedures involve application of the

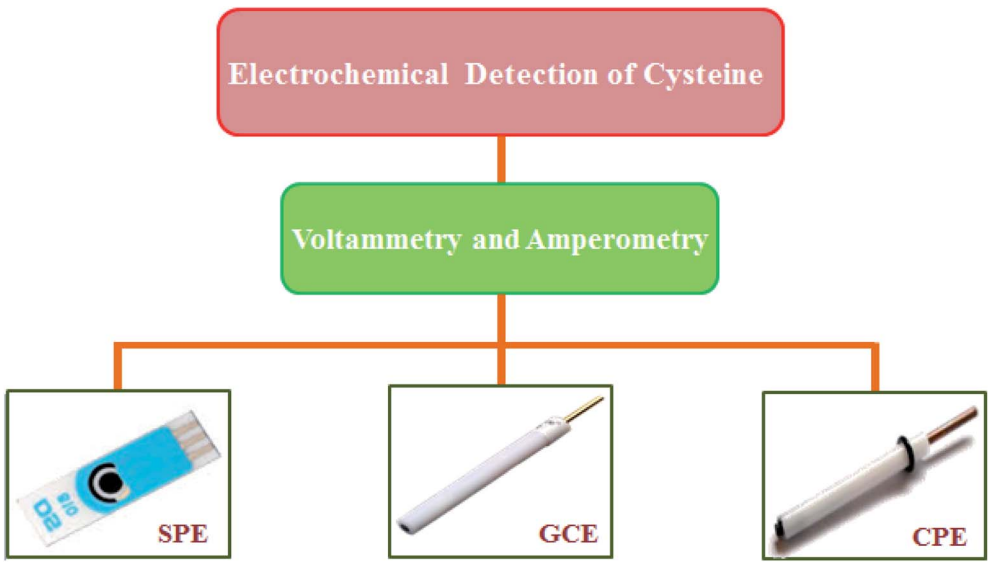

Fig. 1 Schematic illustration of the electrochemical detection of cysteine.

measuring current at distinctive potential points in a current–voltage curve against the constant potential point in the amperometric procedure. Moreover, voltammetry has extensive utilization in trace analyte speciation because of its higher sensitivity and accuracy. It has been considered to be appropriate for partial suppression of the background current and improvement of the limit of detection (LOD). Voltammetry may enable multi-element determination as diverse compounds possess distinct peak potentials. Therefore, qualitative outputs may be observed *via* examination of the reaction of reversibility in the electrochemical cell setup.[35]

Voltammetric techniques, such as differential pulse voltammetry (DPV), cyclic voltammetry (CV), square wave voltammetry (SWV), linear sweep voltammetry (LSV) and so on, are highly appropriate owing to their higher sensitivity, fast analysis times, lower LOD, as well as the affordable equipment required.[36–40] The present review summarizes the recent developments in the voltammetric and amperometric detection of Cys based on a modified carbon paste electrode (CPE), modified glassy carbon electrode (GCE) and modified screen printed electrode (SPE) in the last 6 years (Fig. 1).

Voltammetric and amperometric sensors for the detection of Cys

Voltammetric and amperometric sensors are based on various kinds of substances that enjoy conductive features associated to the transfer of electrons. During recent years, electrochemical detection of Cys has been detected with the use of sensors made from glassy carbon, graphite, graphene (Gr), carbon nanotubes (CNTs), diamond paste, and substances based on metallic nanoparticles (NPs) such as gold (Au), silver-NPs, and so forth. However, metal based electrodes (Au and platinum) suffer from some disadvantages in electroanalytical utilizations, such as low positive potential ranges because the surface is oxidized, a similar procedure takes place in the negative range and the potential overload of the surface of the electrode with impurities increases. A lot of investigations have been conducted on the electrochemical determination of Cys in various modified electrodes containing the metal and metal oxide nanoparticles and their composites, carbon based nanomaterials, ionic liquids, conducting polymers and so on.[41–44] The sensing efficacy of such substances toward Cys improves *via* the use of various strategies, such as adjusting their morphological, structural, chemical, physical, or catalytic features. Moreover, technological progresses in the electrode procurement procedures essentially contribute to the presentation of new options for real-time utilizations.

Voltammetry and amperometry on modified carbon paste electrodes for the determination of Cys

Experts in the field regard carbon as one of the most desirable electrode substrates because it possesses a wide anodic potential range, chemical inertness, a lower residual current, simplified utilization and is affordable. In addition, it exhibits a rapid response time and may be formed into distinct dimensions. Moreover, carbon paste has widespread utilization as the carbon electrode. Furthermore, carbon paste electrodes (CPEs) procured by mixing a graphite powder with insulating liquids such as paraffin oil or silicon oil are one of the most utilized types of working electrode. They have several benefits, for example readily renewable surfaces, affordability, as well as very low background currents, in particular, in the anodic areas.[45,46] However, a caveat of the CPEs is considered to be the tendency of the organic binder for dissolving in the solutions consisting of the organic solvents. At present, a lot of modifications have been observed in these CPEs for improving the electrochemical responses and selectivity towards the analyte. Consequently, biological, as well as chemical, modifications have been considered to be the two key modifications using any of the four processes:[47]

Absorption of the modifier on the electrode surface;
Covalent binding of the modifier to the electrode surface;
Dissolution of the modifier in the pasting liquid, and;
Direct mixing of the modifier with carbon paste.

Therefore, the carbon paste electrode has been one of the most attractive and extensively utilized electrodes for electroanalysis.[48–55]

Benvidi *et al.* prepared a modified CPE on the basis of a synthesized compound 14-(4-hydroxy-phenyl)-14*H*-dibenzo[*a*,*j*]-xanthene (HDX), as well as multi-walled carbon nanotubes (MWCNTs).[56] In the next step, the modified electrode was utilized as an electrochemical sensor to oxidize Cys. Based on the optimal pH, which was equal to 8.5, the overpotential of Cys

Table 1 A number of analytical functions determined for Cys electrochemical detection *via* CPEs modified with different modifiers

Electrochemical sensor	Method	Detection limit	Linear range	Ref.
HBX/MWCNTs/CPE	DPV	1.0 μM	4.0–1000.0 μM	56
DMBQ/ZnO NPs/CPE	SWV	0.05 μM	0.09–340.0 μM	57
Fe_2O_3NPs/N-Gr/CPE	Amperometry	0.1 μM	0.2–400 μM	58
Fe(II)-NX/ZCME	SWV	1.5×10^{-10} M	5.0×10^{-9} to 3.0×10^{-3} M	59
Y_2O_3NPs/N-rGO/CPE	Amperometry	0.8 μM	1.3–720 μM	60
ZnONPs/N-rGO/CPE	Amperometry	0.1 μM	0.1–705.0 μM	61
NiO_xNPs/N-rGO/CPE	Amperometry	0.1 μM	0.3–1620.8 μM	62
MnO_2–TiO_2/DPID/CPE	SWV	0.013 μM	0.025–200.0 μM	63
AF/MgO-NPs/CPE	DPV	30.0 nM	0.1–700.0 μM	64
EFTAG/CPE	SWV	0.9 μM	4.0–2300.0 μM	65

oxidation declined by approximately 280 mV at the modified electrode instead of at the unmodified CPE. The DPV curve for Cys at the electrochemical sensor displayed a LOD of 1.0 μM. Moreover, DPV has been applied to simultaneously determine Cys and tryptophan with the use of an electrochemical sensor. Therefore, this new electrochemical sensor has been employed to determine these substances in real samples; that is, human serum and tablets.

Khalilzadeh *et al.* described the achievement, the electrochemical description, as well as the employment of 8,9-dihydroxy-7-methyl-12*H*-benzothiazolo[2,3-*b*]quinazolin-12-one (DMBQ)/ZnO NPs (ZnO NPs)-CPE (DMBQ/ZnO NPs/CPE) as a modified sensors to electrocatalytically detect Cys in the presence of folic acid.[57] The procured DMBQ/ZnO NPs/CPE were devised as a very sensitive voltammetric sensor to determine Cys in the presence of folic acid in real specimens. The SWV of Cys had a LOD equal to 0.05 μM.

Yang *et al.* fabricated an electrochemical sensor on the basis of Fe_2O_3 NPs supported on N-doped graphene (Fe_2O_3NPs/N-Gr) for electrocatalytic oxidation and detection of L-Cys.[58] The electrochemical behavior of L-Cys at Fe_2O_3NPs/N-Gr has been examined using voltammetry. Therefore, Fe_2O_3NPs/N-GR exhibited a very effective electrocatalytic activity to oxidize L-cysteine in 0.1 M PBS at a pH equal to 7.0. Moreover, the oxidation peak currents increased dramatically at the Fe_2O_3-NPs/N-Gr-modified electrode. Hence, potential utilization of the sensor has been illustrated *via* its use for the analytical detection of L-Cys. Finally, experimental outputs indicated that the electrocatalytic current experienced a linear increase with the L-Cys concentration in a range between 0.2 and 400 μM with the least detectable concentration equal to 0.1 μM.

Hashemi *et al.* constructed an electrochemical sensor using a CPE modified with iron(II) doped with synthesized NPs of zeolite X (Fe(II)-NX/ZCME), which are very sensitive for the detection of Cys.[59] The modified electrode exhibited a very good electroactivity to oxidize Cys in PBS at pH 7.4. Researchers showed that the anodic peak potential of Cys oxidation in comparison to the unmodified CPE shifted towards negative values at the modified electrode surface under optimal conditions. Moreover, the peak current was enhanced linearly with the Cys concentration in a broad range between 5.0×10^{-9} and 3.0×10^{-3} M. In addition, the LOD was low and equal to 1.5×10^{-10} M. In conclusion, the modified electrode was utilized as one of the most selective, simplistic, and exact novel electrochemical sensors to detect Cys in real specimens, such as biological and drug fluids.

Yang *et al.* described an electrochemical sensor for L-Cys based on the utilization of Y_2O_3-NPs supported on nitrogen-doped reduced graphene oxide (N-rGO).[60] Deposited on a CPE, the substance displayed a highly oxidation peak for L-Cys at a pH equal to 7.0 (in comparison with the unmodified electrode). Moreover, the current was measured at a potential of 0.7 V *versus* Ag/AgCl and experienced a linear increase in the concentration range of 1.3–720 μM L-Cys, and the LOD was 0.8 μM. Ultimately, their sensor showed successful utilization for detecting L-Cys in a spiked syrup.

Yang *et al.* synthesized a kind of ZnONPs/N-rGO *via* a low temperature, affordable and one-step hydrothermal procedure. With the use of the procured nanocomposite as a modified electrode substance, an L-Cys electrochemical sensor was fabricated.[61] The nanocomposite showed greater electrocatalytic activities for the oxidation of L-Cys. Based on the optimized detection conditions, the nanocomposite modified electrode showed L-Cys with a wide determination range between 0.1 and 705.0 μM and a LOD equal to 0.1 μM. Finally, the sensor was extensively utilized for determining L-Cys in real specimens.

Yang *et al.* synthesized a new nickel oxide NPs/N-rGO (NiO_xNPs/N-rGO) nanocomposite for the first time, and a NiO_x-NPs/N-rGO modified CPE was fabricated.[62] NiO_xNPs/N-rGO/CPE exhibited very good electro-catalytic activities for the detection of L-Cys in 0.1 M PBS (pH of 10.0). Under optimal conditions, the current responses of L-Cys were linearly enhanced with its concentration between 0.3 and 1620.8 μM so that the lowest detectable concentration was 0.1 μM.

Bananezhad *et al.* presented a modified CPE based on a MnO_2–TiO_2 nanocomposite and 2-(3,4-dihydroxy-phenethyl) isoindoline-1,3-dione (DPID) as a modifier to simultaneously analyze uric acid, Cys, and tryptophan because these are the three major biochemicals in human bodies.[63] The resulting electrode (MnO_2–TiO_2/DPID/CPE) was utilized to examine the electrochemical oxidation of Cys, uric acid and tryptophan. Compared to conventional CPEs, the potential of the oxidation peak of Cys on the MnO_2–TiO_2/DPID/CPE showed a 600 mV decline in the overpotential that can be found at 30 mV and the signals were linear from 0.025 to 200.0 μM. Moreover, a lower LOD equal to 0.013 μM was observed. Finally, MnO_2–TiO_2/DPID/CPE was substantially utilized to concurrently analyze uric acid and Cys, and tryptophan in biological and drug specimens.

Gupta *et al.* studied the effect of the electrical conductivity of MgO-NPs, as well as the electrocatalytic impact of acetylferrocene (AF), to modify CPE as a strongly sensitive electrochemical sensor to electrocatalytically determine L-Cys in an aqueous solution.[64] Therefore, AF/MgO-NPs/CPE exhibited acceptable electrocatalytic activities for the analysis of L-Cys in a concentration range between 0.1 and 700.0 μM with a LOD equal to 30.0 nM with the use of DPV. Additionally, AF/MgO-NPs/CPE had two distinct oxidation signals with a value for the change in energy (ΔE) of approximately 170 mV in the solution, consisting of L-Cys and tryptophan which were found to be adequate to simultaneously detect these amino acids with a similar oxidation potential at the unmodified electrode surface.

In this regard, Beitollahi *et al.* developed a modified CPE on the basis of ethyl 2-(4-ferrocenyl-[1,2,3]triazol-1-yl) acetate (EFTA) and Gr for electrocatalytic oxidation and Cys detection.[65] The electrochemical behavior of Cys at EFTAG/CPE has been examined using voltammetric procedures. It has been found that the oxidation overpotential of Cys declined considerably in comparison to the bare electrode and its oxidation peak currents enhanced remarkably at EFTAGCPE. Moreover, the potential utility of the sensor was shown by using it for the

analytical detection of the Cys concentration. According to the outputs, the electrocatalytic current experienced a linear enhancement with Cys concentrations in the ranges between 4.0 and 2300.0 μM so that the LOD was equal to 0.9 μM. In addition, the procured modified electrode had a very reasonable resolution between the voltammetric peak of tyrosine and Cys. Finally, the sensor was utilized for determining tyrosine and Cys in human fluid specimens. The comparison of several parameters of Cys for all the above mentioned CPEs is summarized in Table 1.

Voltammetry and amperometry on modified glassy carbon electrodes for the determination of Cys

Experts in the field utilized one of the novel forms of carbon called "glassy" carbon as the indicator electrode in voltammetry. In fact, glassy carbon has been considered to be a gas-impermeable, electrically conductive substance with a strong resistance to chemical attack. Therefore, it would be appropriate for use in the potential ranges between almost +1.2 and −0.8 volts *versus* a saturated calomel electrode (SCE) in an acid media.[66] Moreover, GCE has rapid electrokinetics owing to the respective higher electron transfer rate on the surface of the electrode and therefore the response would be more rapid in comparison with the thin-film metals electrode that may be related to the larger diameter of the working area. With regard to its adjustable surface, the GCE can be readily modified by electropolymerizing the inert organic monomers[67] or *via* coating the protecting polymers on the top of the electrode with Nafion. To form a stable bond between Nafion and the surface of GCE, Nafion can be electrochemically or directly applied to the surface.[68] The key benefit of GCE is its probable reutilization *via* polishing of the surface. However, because of the respective physico-chemical features, glassy carbon is one of the most attractive and extensively utilized electrodes, and it has a rather high chemical inertness.[69–77]

Taei *et al.* fabricated a new Au NPs poly(*E*)-4-(*p*-tolyldiazenyl) benzene-1,2,3-triol (Au NPs/PTAT) film GCE (AuNPs/PTAT/GCE) to simultaneously detect the three anti-oxidants Cys, tyrosine and uric acid.[78] The bare GCE could not separate the oxidation peak potential of the molecules, whereas the PTAT film modified electrode could resolve them. In addition, the results of electrochemical impedance spectroscopy (EIS) indicated that the charge transfer resistance of the bare electrode was enhanced as (*E*)-4-(*p*-tolyldiazenyl)benzene-1,2,3-triol was electropolymerized at the bare electrode. In addition, EIS exhibited increased electron transfer kinetics between the electrode and analyte following the electrodeposition of the Au NPs. DPV outputs showed that the electrocatalytic current increased linearly in a range between 2 and 540 μM for Cys, 10 and 560 μM for uric acid, and 5 and 820 μM for tyrosine with a LOD equal to 0.1, 2 and 0.04 μM respectively for uric acid, tyrosine and Cys. Finally, this new technique has been successfully employed for the simultaneous detection of Cys, uric acid and tyrosine in human urine specimens.

Devasenathipathy *et al.* described a GCE modified with AuNPs which have been stabilized using calcium-crosslinked pectin (CCLP) and electrodeposited on the MWCNTs using the chemical vaporization method. Therefore, the resultant electrode has been utilized to selectively determine L-Cys.[79] The electrode description indicated that CCLP functions as one of the scaffolds for forming the strongly stable, smooth and electrochemically active AuNPs. Moreover, electrochemical investigations indicated the MWCNTs significantly promoted the electrodeposition of the CCLP-AuNPs. In addition, the novel GCE had very good electrocatalytic abilities toward L-Cys oxidation, exhibiting a lower overpotential and showing a greater oxidation peak current. Consequently, the diffusion coefficient to oxidize L-Cys was equal to 3.0×10^{-6} cm^2 s^{-1}. Hence, the amperometric sensor displayed a broad linear range between 0.1 and 1000 μM, a higher sensitivity (0.46 μA μM^{-1} cm^{-2}) as well as a LOD equal to 19 nM. As a result, it has been utilized for the specific detection of L-Cys, even in the presence of a 500-fold excess of interferents. Finally, it was found to be stable and possessed a reasonable reproducibility and repeatability, and has been satisfactorily employed for determining L-Cys in spiked specimens of human serum.

Devasenathipathy *et al.* developed a sensitive amperometric sensing platform to detect L-Cys using an iron tetra-sulfonated phthalocyanine (FeTsPc) decorated multi-walled carbon nanotube (MWCNT) composite film modified electrode.[80] The researchers prepared the MWCNT-FeTsPc composite modified GCE, and demonstrated that it possessed a high electrocatalytic function for oxidizing L-Cys with two oxidation peaks, which are related to FeTsPc mediated electrocatalysis. Therefore, the overpotential of the oxidation peaks strongly declined to −0.1 and +0.22 V whereas the peak currents were considerably ameliorated when compared to the control electrode. In addition, an amperometric sensor has been fabricated that had very good electro-analytical variables to determine L-Cys, such as broad linear ranges between 10 μM and 0.2 mM and a lower LOD (1 μM). Moreover, they evaluated the functional ability of their sensor in the human urine specimens. Consequently, this sensor showed a very good repeatability, reproducibility and stability.

Wang *et al.* developed a strongly sensitive and selective electrochemical sensor to detect L-Cys on the basis of a Gr oxide/carboxylated MWCNTs/manganese dioxide/gold NPs composite (GO/CMWCNTs/AuNPs@MnO_2).[81] It should be noted that the feature of GCE that has been modified by GO/CCNTs/AuNPs@MnO_2 involved enhancing the sensing surface areas, as well as the electronic transmission rates. In addition, adding MnO_2 might efficiently ameliorate the specificity and selectivity of L-Cys detection. Therefore, the detection outputs of L-Cys demonstrated a considerable enhancement of the surface area, the sensitivity of the GO/CCNTs/AuNPs@MnO_2 sensor and the electronic transmission rate. In addition, the electrochemical sensor showed a very good stability and reproducibility. Furthermore, L-Cys showed a linear range from 1.0×10^{-8} to 7.0×10^{-6} M and the LOD was equal to 3.4×10^{-9} M. The selectivity results indicated that a 200-fold concentration of ascorbic acid, NH_4^+, Na^+, K^+, Fe^{2+}, SO_4^{2-}, CO_3^{2-} did not affect the determination of Cys. Finally, the proposed electrochemical

sensor was satisfactorily employed for determining trace amounts of L-Cys in spiked water specimens.

In other research, Zheng *et al.* addressed the synthesis of the molybdenum–sulfur nanocube/poly(diallyl dimethyl ammonium chloride)–mesoporous carbon (MoS_2/PDDA–MC) composites using a simplified affordable synthesis strategy that was introduced to design an easy and novel sensitive electrochemical sensor to detect L-Cys.[82] Owing to the larger ratio of the surface to the volume, the higher conductivity of the mesoporous carbon as well as the better biocompatibility of MoS_2, the MoS_2/PDDA-MC-based sensor had very good electrocatalytic activities to detect L-Cys with a broad linear range of 0.45 to 155 μM and a lower LOD of 0.090 μM.

Kaur *et al.* synthesized a highly dispersed Au NPs decorated nanocrystalline zeolite (NanoZSM-5) (AuNPs NanoZSM-5) *via* electrostatic interactions between the functionalized Au NPs, as well as the functionalized nano-crystalline zeolite (Fig. 2). Therefore, they devised an electrochemical sensor on the basis of the Au NPs decorated nano-crystalline zeolite for nanomolar simultaneous determination of Cys and glutathione with a higher sensitivity, as well as a lower LOD.[83] A broad linear range has been observed from 2 nM to 800 μM and 3 nM to 800 μM with a LOD equal to 0.3 and 0.6 nM for Cys and glutathione, respectively. In addition, the AuNPs nano-ZSM-5/GCE showed a high selectivity for the simultaneous determination of Cys and glutathione in the presence of various interfering agents, including L-amino acids (alanine, glycine, arginine, histidine, phenylalanine, proline, tyrosine, valine, tryptophan, glutamic acid, serine, threonine, and methionine), glucose, ascorbic acid, dopamine, and uric acid. In addition, the analytical function of the devised sensor has been verified by determining glutathione and Cys in a commercial drug preparation with acceptable outputs, even in the presence of multiple amino acids.

Wu *et al.* reported the fabrication of an Au NPs–Ni–Al layered double hydroxide (LDH) composite film through a one-step electrochemical deposition on a GCE surface from a mixed solution consisting of $HAuCl_4$ and nitrate salts of Ni^{2+} and Al^{3+}. The results showed a better conductivity with the Au NPs co-deposited on the LDH film. Therefore, the synergic impact of the LDHs and Au NPs remarkably improved the L-Cys electro-oxidation, reflecting the lower oxidation peak potential (0.16 V), as well as higher current responses.[84] Thus, the electrode has been employed for sensing L-Cys, representing a reasonable selectivity and sensitivity.

Mani *et al.* described a simplified electropolymerization procedure for preparing the very stable tetra-amino functionalized cobalt phthalocyanine (pTACoPc) on electrochemically active rGO. Their technique effectively showed the very good physico-chemical features of rGO with the rich redox chemistry of TACoPc. Moreover, GO has been electrochemically reduced to rGO at the electrode surface along with the concomitant electropolymerization of TACoPc. In addition, electrochemical examinations indicated that rGO on the pTACoP/GCE enhanced the efficient surface areas, reduced the charge transfer resistance of the electrodes and augmented the electrochemical signals. In addition, the rGO-pTACoPc film modified electrode exhibited very good electrocatalytic abilities for oxidizing hydrazine and Cys.[85] The preparation of GO and electropolymerization of TACoPc on the rGO for the electrocatalytic

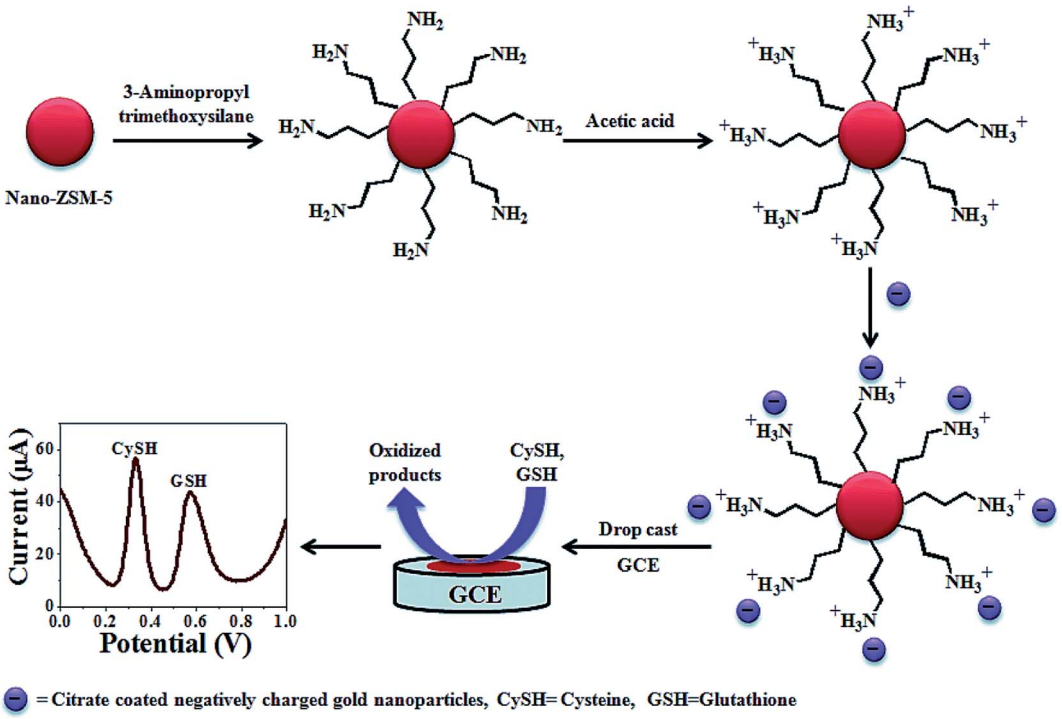

Fig. 2 The construction process of an AuNPs decorated Nano-ZSM-5 based electrochemical sensor. Reproduced with permission from ref. 83. Copyright 2015 Royal Society of Chemistry.

detection of hydrazine and Cys is shown in Fig. 3. To determine Cys, the results showed that the rGO-pTACoPc sensor had a linear concentration range between 50 nM and 2.0 μM, the LOD was equal to 18.5 nM and the sensitivity was equal to 10.19 nA nM^{-1} cm^{-2}. In addition, their sensor showed linear concentration ranges between 50 nM and 2.6 μM, a LOD equal to 10 nM, as well as a sensitivity equal to 1.62 nA nM^{-1} cm^{-2} for determining hydrazine. It is notable that the electrocatalytic abilities of rGO-pTACoPc showed a more acceptable function in comparison to other cobalt phthalocyanine derivatives reported using other methods. Consequently, this novel sensor had a prolonged storage stability, reasonable reproducibility and repeatability. Finally, researchers evaluated the functional utility of the sensor in water and biological specimens.

Geng *et al.* reported a novel, simplified and efficient approach with the use of the hydrothermal reaction, which was followed by increased temperature pyrolysis under ammonia flow for fabrication of the molybdenum nitride nano-sheets/N-doped MWCNTs (MoN/N-MWNTs) hybrid nanocomposite. Fig. 4 shows a schematic diagram of the procurement procedure of the MoN/N-MWNTs nanocomposite. The nanocomposite exhibited very good electrocatalytic oxidation of L-Cys.[86] Moreover, the researchers made an amperometric L-Cys sensor on the basis of the MoN/N-MWNTs modified GCE. Hence, their as-prepared MoN/N-MWNTs nanocomposite had a desirable conductivity, larger surface area, owing to the MWNTs acting as a support, as well as the large exposed active sites of MoN. In addition, the impact of various loading amounts of MoN was determined so that the optimized MoN/N-MWNTs catalyst exhibited a wider detection range, which has been drawn using two line segments (5 μM to 0.79 mM and 0.79 mM to 12.60 mM), a 198.59 nA μM^{-1} cm^{-2} sensitivity in the lower concentration range, a faster response within 1.5 s and finally an acceptable stability and reproducibility.

Shadjou *et al.* fabricated a nanocomposite of Gr quantum dots-β-cyclodextrin on the GCE (GQDs/β-CD/GCE) surface with the use of a one-step, green electro-deposition procedure. The redox of the L-Cys procured by the nanocomposite modified GCE has been described using chronoamperometry, DPV and CV.[87] The modified electrode exhibited effective electrocatalytic activities towards L-Cys oxidation *via* a surface mediated electron transfer. Researchers also showed the catalytic rate constant, as well as the L-Cys diffusion coefficient, and devised a time-saving and sensitive procedure to analyze L-Cys. Finally, their voltammetric technique was employed for determining L-Cys with the use of the Gr quantum dot-β-cyclodextrin-GCE.

Wang *et al.* reported an electrochemical sensor for L-Cys, which contains a GCE modified with a two-dimensional (2D) ternary nanocomposite procured from magnetite, rGO and platinum (known as Pt–Fe_3O_4/rGO).[88] The electrochemical determination procedure has been explored using amperometry, CV, and DPV, as well as double potential step chronoamperometry. Moreover, the diffusion coefficient (7.41×10^{-7} cm^2 s^{-1}) and reaction rate constant (9.96×107 cm^3 mol^{-1}

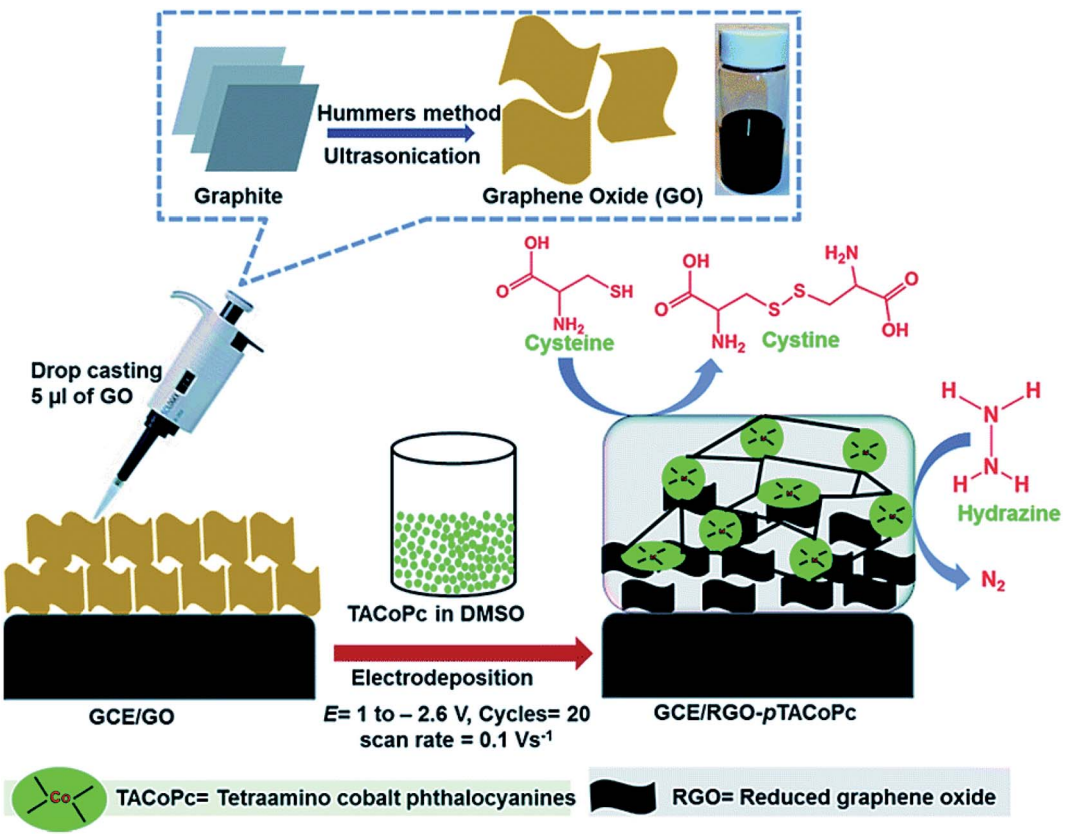

Fig. 3 Preparation of GO and electro-polymerization of TACoPc on RGO to electrocatalytically determine Cys and hydrazine. Reproduced with permission from ref. 85. Copyright 2016 Royal Society of Chemistry.

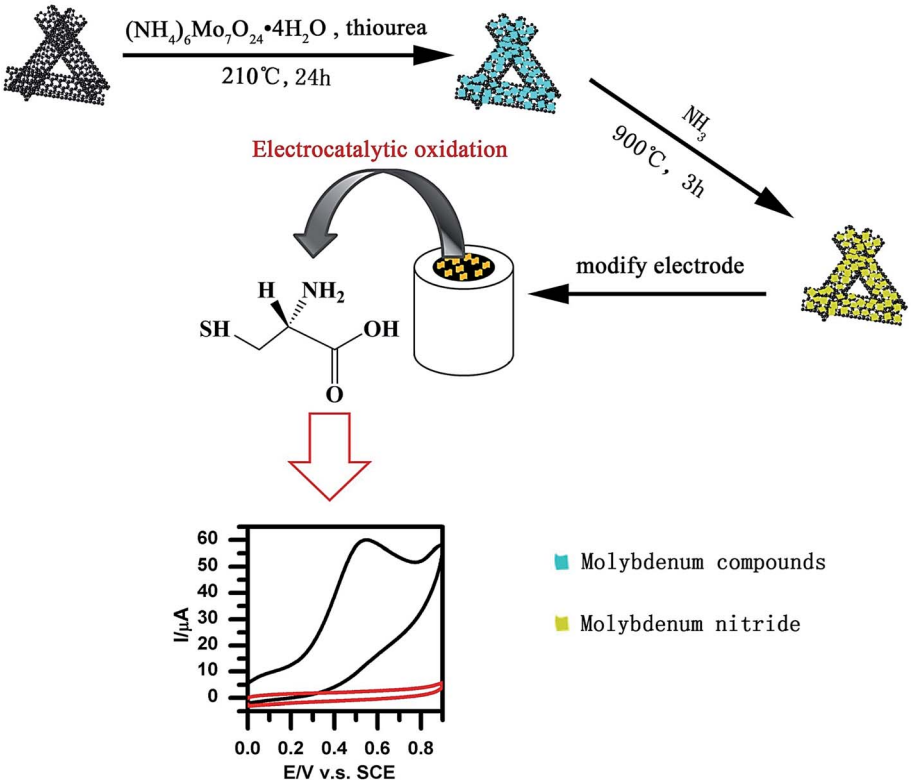

Fig. 4 Preparation of MoN/N-MWNTs nanocomposites. Reproduced with permission from ref. 86. Copyright 2016 Elsevier.

s^{-1}) have been computed by using the Cottrell equation. Therefore, the sensor, which was best operated in 0.1 M NaOH solution at a working voltage equal to 0.65 V *versus* SCE, had a 10 μM LOD and an analytical range between 0.10 and 1.0 mM. This novel sensor demonstrated stability, selectivity, repeatability, and reproducibility owing to the synergistic impact of the diverse elements. Moreover, the LOD was equal to 1.0×10^{-5} M.

Taei *et al.* fabricated a Au NPs/poly-trypan blue modified GCE (AuNPs/poly-TrB/GCE) to simultaneously determine Cys, tyrosine and uric acid (Fig. 5).[89] However, restrictions in the bare GCE were shown in the clear oxidation peaks for uric acid, tyrosine and Cys while the Au NPs/poly-TrB modified electrode could thoroughly isolated the voltammetric signals for uric acid, tyrosine, and Cys at +0.40, +0.58 and +0.90 V *versus* the Ag/AgCl electrode. Moreover, the modified electrode showed very good electrocatalytic activities toward Cys oxidation with a potent shift of approximately 460 mV to a less positive potential. At the optimal experimental conditions, the LOD values for uric acid, tyrosine and Cys were computed as 0.006, 0.07 and 0.008 μM using this simply constructed sensor. Ultimately, this novel sensor has been substantially utilized to simultaneously determine molecules in human biological specimens.

Amini *et al.* proposed an electrochemical sensor to detect L-Cys by immobilizing a poly (alizarin yellow R)/carbon QDs film on a GCE.[90] EIS, CV and amperometry analysis were employed to verify the acceptable step-wise assembly process of the sensor. Moreover, the electro-catalytic behavior of the sensor was examined using amperometry and CV. According to the analysis, the poly(alizarin yellow R)/carbon dots showed considerable electrocatalytic activities to oxidize L-Cys at the optimal condition. It has been also found that the electrocatalytic responses of the sensor were proportionate to the L-Cys concentration in the ranges between 0.3 and 3.6 μM and 3.9 and 7.2 μM with a LOD and sensitivity of 90 nM and 0.482 μA μM^{-1}, respectively.

Amiri *et al.* fabricated magnetic $CoFe_2O_4/SiO_2$ spinel-type nanocomposites using a sol–gel procedure in the presence of various acids. Electrochemical sensor utilization of the nanocrystalline $CoFe_2O_4/SiO_2$ synthesized using salicylic acid for determination of L-Cys has been examined using CV and DPV.[91] Therefore, DPV indicated that the sensor showed a notable sensitivity for the detection of L-Cys. Moreover, the response of a GCE modified with $CoFe_2O_4/SiO_2$ was linear in a concentration range of 0.02–425 μM L-Cys with a LOD equal to 0.20 μM. The electrode produced a partial current response for glutamic acid, citric acid and tryptophan at the applied working potential (+0.748 V *versus* Ag/AgCl). The electrode demonstrated reliability, simplicity, a rapid preparation time, and accuracy, with no need for additional sample treatment.

Yusoff *et al.* described an amperometric sensor for L-Cys that contains a GCE, which has been modified with rGO within the Nafion film and decorated with PdNPs.[92] The modified GCE gave linear electro-oxidative responses to L-Cys (typically at +0.6 V *vs.* SCE) in a concentration range of 0.5 to 10 μM. Moreover, they had advantages such as a response time of less than 2 s, a 0.15 μM LOD, as well as an analytical sensitivity of

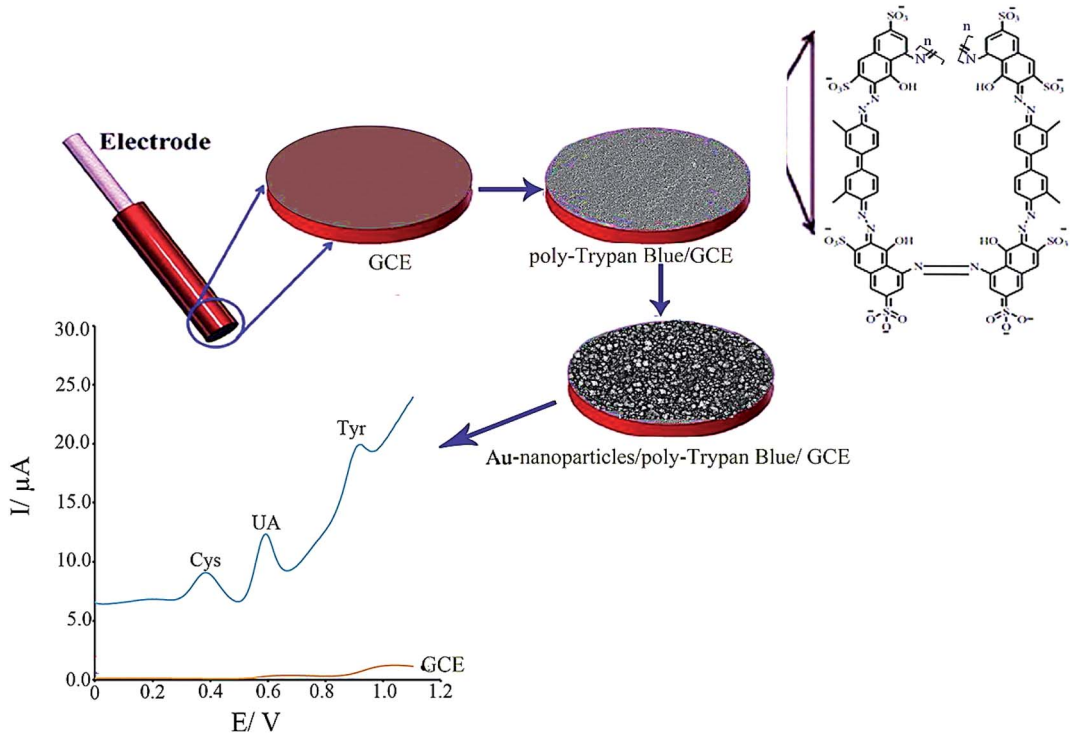

Fig. 5 Schematic illustration of the fabrication of AuNPs/poly-TrB/GCE for electrochemical sensing of cysteine. Reproduced with permission from ref. 89. Copyright 2017 Elsevier.

1.30 μA μM^{-1} cm^{-2}. The sensor displayed selectivity over uric acid, ascorbic acid, hydrogen peroxide, dopamine, glucose and urea. Finally, the modified GCE was utilized for the detection of L-Cys in human urine specimens, and showed a very good recovery.

Ziyatdinova *et al.* developed an electrochemical sensor based on poly(*p*-coumaric acid) electro-deposited over the surface of a MWCNTs modified GCE (poly(*p*-coumaric acid)/MWNT/GCE) to directly determine L-Cys.[93] Poly(*p*-coumaric acid) was observed using potentiodynamic electrolysis based on the optimal conditions (0.10 mM *p*-coumaric acid in 0.1 M NaOH with the use of five cycles in a potential window equal to 0–1.0 V and a scan rate equal to 25 mV s^{-1}), which provided the greatest voltammetric response that was equal to the concentration of L-Cys. The porous structure of the polymeric film provided a 6.9-fold enhancement in the efficient surface area and a 4.2-fold lower charge transfer resistance compared with the GCE. The DPV results reveal the sensor response is linear in the range between 7.5–50 and 50–1000 μM of L-Cys with LOD and limit of quantitation (LOQ) values equal to 1.1 and 3.6 μM. Researchers found a very high selectivity to L-Cys in the presence of uric acid, ascorbic acid, glucose, L-tyrosine, dopamine, and S-containing materials (glutathione, homocysteine, L-cystine, α-lipoic acid and L-methionine). The usability of the sensor for real sample analyses has been observed in human urine.

Yang *et al.* fabricated their own sensitive molecularly imprinted sensor to detect L-Cys using the electrodeposition method.[94] The molecularly imprinted polymer (MIP) film was procured *via* the electrodeposition of chitosan in the presence of Cys following the deposition of nanoporous gold (np-Au) and CuNPs over a GCE surface. Therefore, the MIP/CuNPs/np-Au/GCE sensor has been described using EIS and CV. Hence, the sensor exhibited a very good recognition for Cys by measuring the variation in the oxidation current of Cys. According to the analyses, the current response was linear for the analyte logarithm concentration in ranges between 0.5 nM and 10 μM, with a LOD equal to 0.7×10^{-10} M. In addition, the selectivity results demonstrated that L-histidine, L-tryptophan, L-tyrosine, L-dopamine, L-ascorbic acid, and uric acid have little effect on the determination of Cys. The procured sensor has been satisfactorily utilized for determining Cys in bovine serum and in the sauce from instant noodle specimens with a reasonable recovery in a range between 93.0 and 110.0%. Finally, favorable functions can be ascribed to the synergic catalytic effects and larger surface areas of the CuNPs/np-Au nanocomposites.

Li *et al.* prepared a multilayered catalyst based on rGO and poly [1-vinyl-3-ethyl-imidazolium bis(trifluoromethanesulfonyl) amide][Veim] [TFSA] with a higher loading capacity to immobilize the Ag NPs. In addition, a poly(ionic liquids) (PIL), rGO nanocomposite has been procured using a mini-emulsion polymerization procedure. Functionalizing the rGO with PIL prevents the metal leaching because the PIL–rGO nanocomposite offers some of the particular binding sites necessary for anchoring and growing the silver NPs on the rGO surface. In addition, for the first time, a nonenzymatic L-Cys sensor has been made on the basis of the final nano-hybrid.[95] Finally, the modified sensor presented interesting analytical characteristics, such as super electrocatalytic activities, a notable LOD (6 nM), and wider detection ranges between 0.1 and 500 μM. In addition, the selectivity studies indicated that the AgNPs–PIL–

rGO/GCE has a very good selectivity for Cys detection in the presence of homocystine, glutathione, tryptophan, glucose, cystine, vitamin C, uric acid and phenylalanine.

For the first time, Prabhu *et al.* synthesized a mononuclear cobalt(II) tetra[4-(2-{(*E*)-[(4-bromophenyl)imino]methyl} phenoxy)] phthalocyanine (CoTBrImPc) complex. According to the analysis, the synthesized phthalocyanine complex was electrochemically active and immobilized on GCE using a drop-casting technique and was utilized to detect L-Cys.[96] Moreover, the CoTBrImPc modified electrode acted as an acceptable electrocatalyst to the catalytic oxidation of L-Cys with a shift in the over-potential towards the less positive potential and an increased catalytic current in comparison with the bare GCE. In addition, a linear response has been obtained to voltammetrically detect L-Cys in a concentration range between 10 and 100 nM with a coefficient of regression of $R^2 = 0.9993$, a LOD equal to 3 nM and a sensitivity of 2.99 μA nM^{-1} cm^{-2}. Furthermore, the amperometric sensor that was designed to detect L-Cys revealed linear responses in a concentration range similar to the range of CV with a linear equation $y = 0.7582x + 16.9535$ and a correlation coefficient of $R^2 = 0.9961$. Consequently, the LOQ and LOD values for the amperometric determination were equal to 4 and 12 nM with a 10.81 μA nM cm^{-2} sensitivity.

Rasheed *et al.* reported the sensitive electrochemical detection of L-Cys based on a highly stable Pd@$Ti_3C_2T_x$ (MXene) nanocomposite modified GCE (Fig. 6).[97] The MXene acts as the conductive matrix and a reducing agent at the electrode surface, and the Pd NPs are there to improve the stability of $Ti_3C_2T_x$ and to enhance the electrocatalytic activity towards L-Cys detection. The Pd@$Ti_3C_2T_x$/GCE sensor exhibited a detection limit of 0.14 μM and a linear electro-oxidative response to L-Cys within the concentration range from 0.5 to 10 μM. The sensor also demonstrated excellent selectivity over common interfering ions such as ascorbic acid, uric acid, dopamine, and glucose.

Atacan *et al.* developed an electrochemical sensor based on a GCE modified $CuFe_2O_4$/rGO nano-composite decorated with Au NPs for the electrochemical determination of L-Cys.[98] Fig. 7 shows a schematic diagram of the synthesis procedure for GO (1), $CuFe_2O_4$/rGO (2) and $CuFe_2O_4$/rGO–Au (3). The electrochemical description of the modified and bare glassy carbon electrodes (GCEs) was performed using EIS and CV. Moreover, modifying the GCEs enhanced the surface area. Therefore, $CuFe_2O_4$/rGO–Au showed a very effective electrocatalytic activity to oxidize L-Cys in 0.1 M PBS at a pH of 6.5 and a greater sensitivity of 100.01 μA mM^{-1} cm^{-2}. Finally, the electrocatalytic current was augmented linearly with an L-Cys concentration in the range of 0.05 to 0.2 mM with a LOD of 0.383 μM.

A comparison of several parameters of Cys for all of the above mentioned GCEs is summarized in Table 2.

Voltammetry and amperometry on modified SPEs for the determination of Cys

The published research demonstrates that since the 1990s, screen printing technology has been adapted from the microelectronics industry for the high volume generation of very cheap, and yet largely reliable and reproducible, single use sensors that are one of the techniques that have promise for future on-site monitoring. Hence, researchers have been highly attracted by the utilization of screen printing technology in the serial generation of disposable affordable electrodes to electrochemically determine a broad range of materials.[99] In fact, screen printed electrodes (SPEs) are considered to be tools generated by printing various inks on diverse kinds of ceramic or plastic substrates. Moreover, polyester screens are usually employed to print the patterns designed by the analyst with respect to analytical purposes. In addition, the composition of the diverse inks used to print on the electrodes determines the sensitivity and selectivity necessary for all analyses. In other words, various examples of these tools have been reported in the market. Electrochemical determination using SPEs has widespread applications in biomedical and clinical areas for the detection of biological molecules.[100–102] In addition to the simplified modification procedures, SPEs possess the following features, robustness, disposability, rapidness, affordability, trace volume consumption, higher reproducibility, as well as low sample pre-treatment requirements. These features result in their potential future use as detection tools in complicated matrices.[103,104] Therefore, SPEs may be satisfactorily utilized for

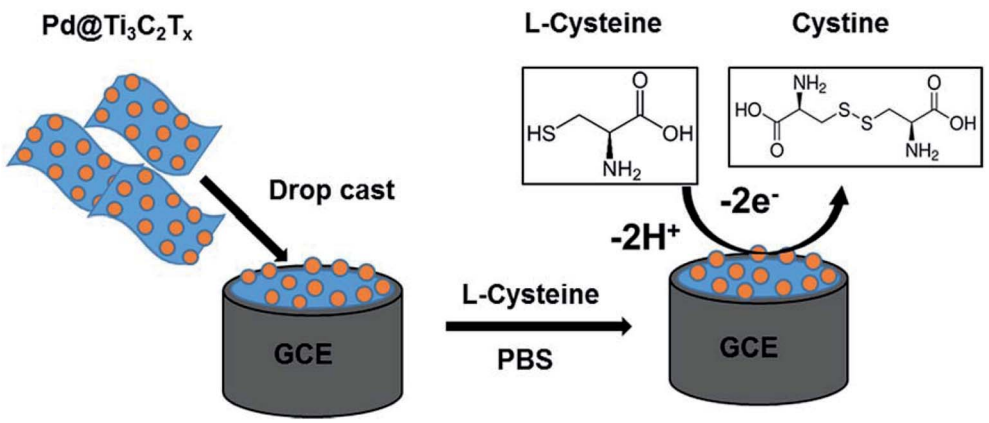

Fig. 6 Schematic diagram of the fabrication of the Pd@$Ti_3C_2T_x$ composite electrode and sensing protocol based on the oxidation of L-Cys at the Pd@$Ti_3C_2T_x$ modified electrode. Reproduced with permission from ref. 97. Copyright 2019 Royal Society of Chemistry.

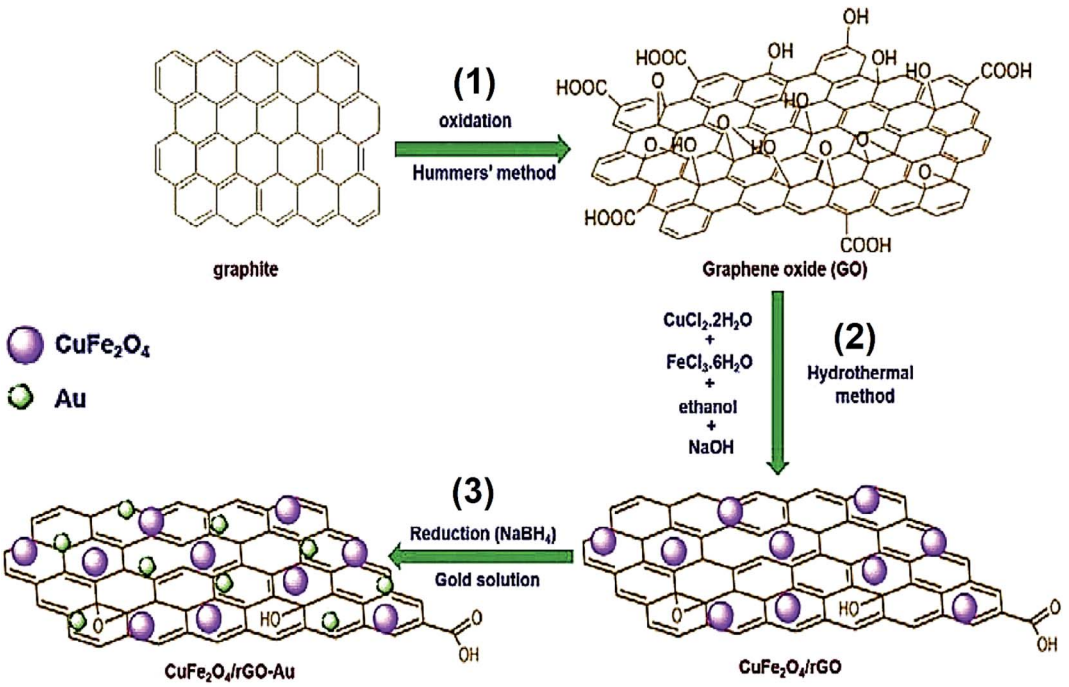

Fig. 7 Synthesis process of (1) GO, (2) $CuFe_2O_4$/rGO, and (3) $CuFe_2O_4$/rGO–Au. Reproduced with permission from ref. 98. Copyright 2019 Elsevier.

Table 2 A number of analytical functions determined for Cys electrochemical detection *via* GCEs modified with different modifiers

Electrochemical sensor	Method	Detection limit	Linear range	Ref.
AuNPs/PTAT/GCE	DPV	0.04 μM	2–540 μM	78
MWCNT/CCLP–AuNPs/GCE	Amperometry	19 nM	0.1 to 1000 μM	79
MWCNT–FeTsPc/GCE	Amperometry	1 μM	10 μM–0.2 mM	80
GO/CMWCNTs/AuNPs@MnO_2/GCE	DPV	3.4×10^{-9} M	1.0×10^{-8} to 7.0×10^{-6} M	81
MoS_2/PDDA-MC/GCE	Amperometry	0.090 μM	0.45–155 μM	82
AuNPs-nano-ZSM-5/GCE	DPV	0.3 nM	2 nM–800 μM	83
Au NPs–Ni–Al LDH/GCE	DPV	6.0 mM	10.0 μM–1.0 mM	84
rGO-pTACoPc/GCE	Amperometry	18.5 nM	50 nM–2.0 μM	85
MoN/N-MWNTs/GCE	Amperometry	3.64 μM	5 μM–0.79 mM	86
GQDs/β-CD/GCE	DPV	—	0.01 to 2 mM	87
Pt–Fe_3O_4/rGO/GCE	DPV	10 μM	0.10–1.0 mM	88
AuNPs/poly-TrB/GCE	DPV	0.006 μM	5.0–270.0 μM	89
Carbon QDs/alizarin yellow/GCE	Amperometry	0.09 μM	0.3–7.2 μM	90
$CoFe_2O_4$/SiO_2/GCE	DPV	0.20 μM	0.02–425 μM	91
rGO-Nafion@Pd/GCE	Amperometry	0.15 μM	0.5–10 μM	92
poly(*p*-coumaric acid)/MWNT/GCE	DPV	1.1 μM	7.5–1000 μM	93
MIP/CuNPs/np-Au/GCE	DPV	0.7×10^{-10} M	0.5 nM–10 μM	94
AgNPs–PIL–rGO/GCE	DPV	6 nM	0.1–500 μM	95
CoTBrImPc/GCE	CV	3 nM	10–100 nM	96
	Chronoamperometry	4 nM	10–80 nM	
Pd@$Ti_3C_2T_x$/GCE	Amperometry	0.14 μM	0.5–10 μM	97
$CuFe_2O_4$/rGO–Au/GCE	CV	0.383 μM	0.05–0.2 mM	98

in situ analyses and improved detection, as has been demonstrated during recent years.[105–108]

Hernández-Ibáñez *et al.* proposed an electrochemical sensor to accurately provide the electroanalytical detection of L-Cys on the basis of a Co(II)-phthalocyanine NP bulk modified disposable SPE (CoPc-SPE).[109] Therefore, they used SWV and CV to reveal the very good electro-catalytic activity towards the electrochemical oxidation of L-Cys with the use of CoPc-SPEs in the optimum neutral or basic pH. In addition, the SWV response of L-Cys exhibited linear ranges between 2.6 and 200 μM with a lower LOD that was equal to 4 μM and a sensitivity of 0.750 μA cm^{-2} μM^{-1}. Moreover, the CoPc-SPE platforms displayed a beneficial reproducibility, and thus the effect of innate interferences like amino acids has been assessed. Finally, the

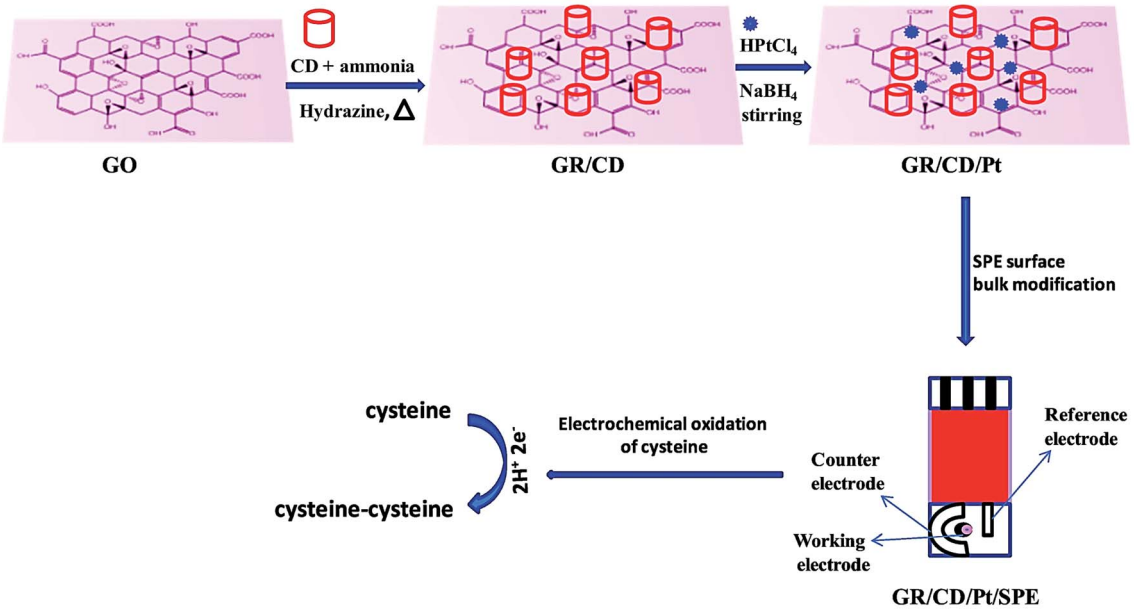

Fig. 8 Schematic representation of sensor fabrication (GR/CD/Pt/SPE). Reproduced with permission from ref. 110. Copyright 2018 Elsevier.

usability of the L-Cys electrochemical sensor on the basis of the CoPc-SPEs was satisfactorily utilized for the first time to evaluate L-Cys in a complex embryo cell culture medium.

Singh *et al.* presented a specific and sensitive sensing platform to determine Cys. In order to make an electrochemical sensor, the rGO–β-cyclodextrin–Pt nanocomposite (rGO/CD/Pt) was procured and the SPE surface was bulk-modified with this nanocomposite, showing very good electrocatalytic activities towards Cys sensing (Fig. 8).[110] In addition, the electrochemical behaviors of the constructed sensor have been examined using DPV and CV, as well as EIS. In the course of Cys detection, a reasonable electrocatalytic response current was observed that was linear considering the Cys concentration in a range from 0.5 to 170 μM with a LOD of 0.12 μM.

Cao *et al.* also devised an L-Cys electrochemical sensor based on CeO_2 nanofibers modified screen printed carbon electrodes (SPCEs).[111] The electrochemical, as well as the electrocatalytic, functions of the CeO_2 nano-fibers modified SPCEs were assessed with the use of CV and amperometry. According to the experimental outputs, the CeO_2 nano-fibers modified SPCEs had very good electrocatalytic activities towards L-Cys detection. In particular, their electrochemical sensor had a higher sensitivity equal to 120 mA mM^{-1} cm^{-2}, a low LOD of 0.02 μM and a wider linear range up to 200 mM for the determination of L-Cys, these are considered to be the most reasonable values. Additionally, the researchers revealed an acceptable selectivity and higher inter- and intra-electrode reproducibility. Finally, this novel L-Cys sensor was utilized to detect L-Cys spiked in human serum specimens with an increased accuracy.

Another study conducted by Kurniawan *et al.* designed a disposable L-Cys sensor on the basis of the SPAuE electrodeposited with copper.[112] The preparation of the disposable Cu/SPAuE sensing platform is shown in Fig. 9. The fixed potential electrodeposition was performed at −0.4 V (*vs.* an Ag

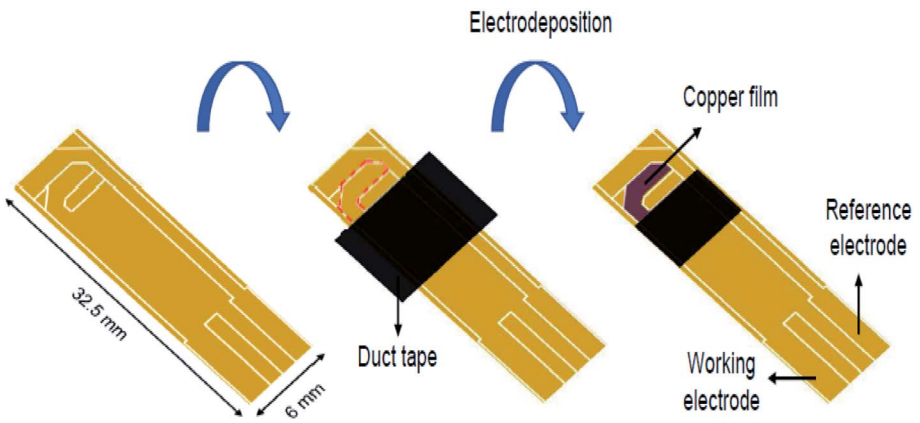

Fig. 9 Schematic diagram of the preparation of a disposable Cu/SPAuE for use as a Cys sensing platform. Reproduced with permission from ref. 112. Copyright 2018 Elsevier.

Table 3 A number of analytical functions determined for Cys electrochemical detection *via* SPEs modified with different modifiers

Electrochemical sensor	Method	Detection limit	Linear range	Ref.
CoPc-SPE	SWV	2.6–200 μM	4 μM	109
rGO/CD/Pt/SPE	DPV	0.12 μM	0.5–170 μM	110
CeO_2 nanofibers/SPCE	Amperometry	0.02 μM	Up to 200 μM	111
Cu/SPAuE	Amperometry	0.21 μM	1–1800 mM	112

pseudo-reference) for 480 s. Then, the crystal structure and morphology of the electro-deposited copper were explored *via* scanning electron microscopy (SEM) and X-ray diffraction. Moreover, the analytical usability of the copper-modified SPAuE (Cu/SPAuE) was assessed in an alkaline medium to electro-oxidize L-Cys with the use of amperometry and CV procedures. According to the analysis, Cu/SPAuE showed a quick response time (<5 s) and two linear ranges between 1 and 400 μM (0.028 mA mM^{-1} sensitivity) and 400 to 1800 μM (0.014 μA μM^{-1} sensitivity) with a LOD of 0.21 μM. In addition, the novel L-Cys sensor exhibited a higher specificity in the presence of conventional interfering electroactive substances such as oxalic acid, glucose, sucrose, urea, citric acid, uric acid and EDTA. Consequently, they demonstrated the successful application of their method for determining L-Cys in human and rabbit blood serum without any sample pre-treatment and the analytical recovery was acceptable.

The comparison of several parameters of Cys for all of the above mentioned SPEs is summarized in Table 3.

Conclusions and perspectives

The present review provides a summary of a number of the current voltammetric and amperometric detection methods for Cys, because it is necessary to utilize quick procedures for determining Cys levels from diverse specimens. It is notable that electrochemical sensors have been based on CPE, GCE and SPE modified with different electrocatalytic materials. Experts in the field have examined various electrocatalytic substances such as carbon based substances, metal and metal oxide NPs, polymers, and so on as modifiers of conventional electrodes. Moreover, they have employed electrochemical platforms with diverse electrochemical procedures to detect Cys with a greater selectivity and sensitivity, wider dynamic ranges and lower LOD values. Comparison of the LOD and the linear concentration range of the observed outputs described in the text are presented and briefly illustrated in Tables 1–3 for comparison. Electrochemical analysis is a quick way to detect Cys. However, commonly used commercial electrodes are subject to electrocatalytic performance limitations, and the poor specificity is not applicable to direct quantification. As a result, electrode surface modification is the main aspect of the successful electrochemical detection of Cys. Although the performance of modified electrodes for Cys detection has been significantly improved, challenges still exist for further investigations using electrochemical Cys sensors. The performance (LOD and linear range) is still poor compared to the results of fluorescence methods and high performance liquid chromatography (HPLC). Therefore, future research needs to focus on the study and synthesis of electrocatalytic materials, especially nano substances with larger surface areas, and a higher conductivity, as well as a uniform dispersion, to improve the catalytic performance for the electrochemical detection of Cys.

Conflicts of interest

There are no conflicts to declare.

Acknowledgements

This research was supported by the National Research Foundation of Korea (NRF) funded by the Ministry of Science and ICT (2020M2D8A206983011). Furthermore, financial support from the Basic Science Research Program (2017R1A2B3009135) through the National Research Foundation of Korea is appreciated.

References

1 Y. Song, C. Xu, H. Kuroki, Y. Liao and M. Tsunoda, *J. Pharm. Biomed. Anal.*, 2018, **147**, 35.
2 F. Cao, Y. Huang, F. Wang, D. Kwak, Q. Dong, D. Song, J. Zeng and Y. Lei, *Anal. Chim. Acta*, 2018, **1019**, 103.
3 Y. Dong and J. Zheng, *J. Mol. Liq.*, 2014, **196**, 280.
4 M. N. Abbas, A. A. Saeed, B. Singh, A. A. Radowan and E. Dempsey, *Anal. Methods*, 2015, **7**, 2529.
5 X. Wang, C. Luo, L. Li and H. Duan, *J. Electroanal. Chem.*, 2016, **757**, 100.
6 B. Alessandro, E. A. Amy, F. M. Dale, P. Maria, R. Michael, J. S. Larry and C. Michael, *J. Biol. Chem.*, 1998, **273**, 22498.
7 J. L. Hammond, A. J. Gross, P. Estrela, J. Iniesta, S. J. Green, C. P. Winlove, P. G. Winyard, N. Benjamin and F. Marken, *Anal. Chem.*, 2014, **86**, 6748.
8 D. Z. Yuan, D. Z. Wei, M. L. Qing and C. Hong, *Sens. Actuators, B*, 2003, **92**, 279.
9 M. Suzanne and T. Nyokong, *J. Electroanal. Chem.*, 2000, **492**, 120.
10 G. Shenguang, Y. Mei, L. Juanjuan, Z. Meng, Y. Feng, Y. Jinghua, S. Xianrang and Y. Shilin, *Biosens. Bioelectron.*, 2012, **31**, 49.
11 M. T. Heafield, S. Fearn, G. B. Steventon, R. H. Waring, A. C. Williams and S. G. Sturman, *Neurosci. Lett.*, 1990, **110**, 216.
12 T. D. Nolin, M. E. McMenamin and J. Himmelfarb, *J. Chromatogr. B: Anal. Technol. Biomed. Life Sci.*, 2007, **852**, 554.

13 Y. Wang, J. Lu, L. Tang, H. Chang and J. Li, *Anal. Chem.*, 2009, **81**, 9710.
14 X. Chen, H. Liu, C. Wang, H. Hu, Y. Wang, X. Zhou and J. Hu, *Talanta*, 2015, **138**, 144.
15 Y. Wang, J. Wang, F. Yang and X. Yang, *Anal. Sci.*, 2010, **26**, 545.
16 S. Chen, H. Gao, W. Shen, C. Lu and Q. Yuan, *Sens. Actuators, B*, 2014, **190**, 673.
17 D. O. Perevezentseva and E. V. Gorchakov, *J. Solid State Electrochem.*, 2012, **16**, 2405.
18 X. Liu, L. Luo, Y. Ding, Z. Kang and D. Ye, *Bioelectrochemistry*, 2012, **86**, 38.
19 A. A. Kumar, B. K. Swamy, T. S. Rani, P. S. Ganesh and Y. P. Raj, *Mater. Sci. Eng., C*, 2019, **98**, 746.
20 S. Tajik, H. Beitollahi, F. Garkani Nejad, M. Safaei, K. Zhang, Q. V. Le, R. S. Varma, H. W. Jang and M. Shokouhimehr, *RSC Adv.*, 2020, **10**, 21561.
21 M. A. Deshmukh, R. Celiesiute, A. Ramanaviciene, M. D. Shirsat and A. Ramanavicius, *Electrochim. Acta*, 2018, **259**, 930.
22 S. Tajik, H. Beitollahi, M. R. Aflatoonian, B. Mohtat, B. Aflatoonian, I. Sheikh Shoaie, M. A. Khalilzadeh, M. Ziasistani, K. Zhang, H. W. Jang and M. Shokouhimehr, *RSC Adv.*, 2020, **10**, 15171.
23 S. He, P. He, X. Zhang, X. Zhang, K. Liu, L. Jia and F. Dong, *Anal. Chim. Acta*, 2018, **1031**, 75.
24 M. R. Aflatoonian, S. Tajik, B. Mohtat, B. Aflatoonian, I. Sheikh Shoaie, H. Beitollahi, K. Zhang, H. W. Jang and M. Shokouhimehr, *RSC Adv.*, 2020, **10**, 13021.
25 P. Balasubramanian, R. Settu, S. M. Chen, T. W. Chen and G. Sharmila, *J. Colloid Interface Sci.*, 2018, **524**, 417.
26 S. Tajik, H. Beitollahi, S. Zia Mohammadi, M. Azimzadeh, K. Zhang, Q. V. Le, Y. Yamauchi, H. W. Jang and M. Shokouhimehr, *RSC Adv.*, 2020, **10**, 30481.
27 V. H. R. Azevedo, J. L. da Silva and N. R. Stradiotto, *J. Electroanal. Chem.*, 2019, **845**, 57.
28 H. Soltani, H. Beitollahi, A. H. Hatefi-Mehrjardi, S. Tajik and M. Torkzadeh-Mahani, *Anal. Bioanal. Electrochem.*, 2014, **6**, 67–79.
29 N. S. Anuar, W. J. Basirun, M. Shalauddin and S. Akhter, *RSC Adv.*, 2020, **10**, 17336.
30 M. M. Motaghi, H. Beitollahi, S. Tajik and R. Hosseinzadeh, *Int. J. Electrochem. Sci.*, 2016, **11**, 7849.
31 Q. He, J. Liu, X. Liu, G. Li, P. Deng and J. Liang, *Colloids Surf., B*, 2018, **172**, 565.
32 S. Tajik, H. Beitollahi, F. Garkani Nejad, K. Zhang, Q. V. Le, H. W. Jang, S. Y. Kim and M. Shokouhimehr, *Sensors*, 2020, **20**, 3364.
33 A. Shah, A. Nisar, K. Khan, J. Nisar, A. Niaz, M. N. Ashiq and M. S. Akhter, *Electrochim. Acta*, 2019, **321**, 134658.
34 F. Arduini, C. Majorani, A. Amine, D. Moscone and G. Palleschi, *Electrochim. Acta*, 2011, **56**, 4209.
35 B. Bansod, T. Kumar, R. Thakur, S. Rana and I. Singh, *Biosens. Bioelectron.*, 2017, **94**, 443.
36 H. Beitollahi, S. Tajik, Z. Dourandish, K. Zhang, Q. V. Le, H. W. Jang, S. Y. Kim and M. Shokouhimehr, *Sesnors*, 2020, **20**, 3256.
37 M. Beytur, F. Kardaş, O. Akyıldırım, A. Özkan, B. Bankoğlu, H. Yüksek, M. L. Yola and N. Atar, *J. Mol. Liq.*, 2018, **251**, 212.
38 H. Beitollahi, M. Safaei and S. Tajik, *Anal. Bioanal. Chem. Res.*, 2019, **6**, 81.
39 A. Wong, A. M. Santos and O. Fatibello-Filho, *Sens. Actuators, B*, 2018, **255**, 2264.
40 P. Balasubramanian, T. S. T. Balamurugan, S. M. Chen, T. W. Chen and P. H. Lin, *Sens. Actuators, B*, 2019, **283**, 613.
41 M. C. Gallo, B. M. Pires, K. C. Toledo, S. A. Jannuzzi, E. G. Arruda, A. L. Formiga and J. A. Bonacin, *Synth. Met.*, 2014, **198**, 335.
42 X. Tang, Y. Liu, H. Hou and T. You, *Talanta*, 2010, **80**, 2182.
43 Z. Mo, F. Zhao, F. Xiao and B. Zeng, *J. Solid State Electrochem.*, 2010, **14**, 1615.
44 Y. P. Hsiao, W. Y. Su, J. R. Cheng and S. H. Cheng, *Electrochim. Acta*, 2011, **56**, 6887.
45 I. Švancara, A. Walcarius, K. Kalcher and K. Vytřas, *Cent. Eur. J. Chem.*, 2009, **7**, 598.
46 J. Wang, *Analytical Electrochemistry*. John Wiley & Sons Inc., NJ, USA. 2006.
47 K. Kalcher, *Electroanalysis*, 1990, **2**, 419.
48 S. Tajik, M. A. Taher, Sh. Jahani and M. Shanehsaz, *Anal. Bioanal. Electrochem.*, 2016, **8**, 899.
49 M. D. C. Teixeira, F. S. Felix, S. S. Thomasi, Z. M. Magriotis, J. M. da Silva, L. L. Okumura and A. A. Saczk, *Microchem. J.*, 2019, **148**, 66.
50 Y. Liu, T. Li, C. Ling, Z. Chen, Y. Deng and N. He, *Chin. Chem. Lett.*, 2019, **30**, 2211.
51 H. Beitollahi, H. Karimi-Maleh and H. Khabazzadeh, *Anal. Chem.*, 2008, **80**, 9848.
52 G. Manasa, A. K. Bhakta, Z. Mekhalif and R. J. Mascarenhas, *Electroanalysis*, 2019, **31**, 1363.
53 H. Mahmoudi-Moghaddam, S. Tajik and H. Beitollahi, *Microchem. J.*, 2019, **150**, 104085.
54 G. Manasa, A. K. Bhakta, Z. Mekhalif and R. J. Mascarenhas, *Mater. Sci. Energy Technol.*, 2020, **3**, 174.
55 S. M. Foukmeniok, O. Ilboudo, E. Njanja, I. Tapsoba, M. Pontie and I. T. Kenfack, *J. Appl. Electrochem.*, 2019, **49**, 575.
56 A. Benvidi, M. M. Ansaripour, N. Rajabzadeh, H. R. Zare and B. B. F. Mirjalili, *Anal. Methods*, 2015, **7**, 3920.
57 M. A. Khalilzadeh, H. Karimi-Maleh and V. K. Gupta, *Electroanalysis*, 2015, **27**, 1766.
58 S. Yang, G. Li, G. Wang, D. Deng and L. Qu, *J. Solid State Electrochem.*, 2015, **19**, 3613.
59 H. S. Hashemi, A. Nezamzadeh-Ejhieh and M. Karimi-Shamsabadi, *Mater. Sci. Eng., C*, 2016, **58**, 286.
60 S. Yang, G. Li, Y. Wang, G. Wang and L. Qu, *Microchim. Acta*, 2016, **183**, 1351.
61 S. Yang, G. Li, C. Qu, G. Wang and D. Wang, *RSC Adv.*, 2017, **7**, 35004.
62 S. Yang, G. Li, L. Liu, G. Wang, D. Wang and L. Qu, *J. Alloys Compd.*, 2017, **691**, 834.
63 A. Bananezhad, H. Karimi-Maleh, M. R. Ganjali and P. Norouzi, *Electroanalysis*, 2018, **30**, 1767.

64 V. K. Gupta, Z. Shamsadin-Azad, S. Cheraghi, S. Agarwai, M. A. Taher and F. Karimi, *Int. J. Electrochem. Sci.*, 2018, **13**, 4309.
65 H. Beitollahi, M. R. Ganjali, P. Norouzi, K. Movlaee, R. Hosseinzadeh and S. Tajik, *Measurement*, 2020, **152**, 107302.
66 H. E. Zittel and F. J. Miller, *Anal. Chem.*, 1965, **37**, 200.
67 K. Pandi, M. Sivakumar, S. M. Chen, M. Sakthivel, G. Raghavi, T. W. Chen, Y. C. Liu and R. Madhu, *J. Electrochem. Soc.*, 2018, **165**, B469.
68 A. Liao, P. Li, H. Zhang, M. Guo, Y. Xia, Z. Li and W. Huangz, *J. Electrochem. Soc.*, 2017, **164**, H63.
69 M. L. Yola and N. Atar, *Mater. Sci. Eng., C*, 2019, **96**, 669.
70 L. Fu, A. Wang, G. Lai, C. T. Lin, J. Yu, A. Yu, Z. Liu, K. Xie and W. Su, *Microchim. Acta*, 2018, **185**, 87.
71 M. R. Ganjali, H. Beitollahi, R. Zaimbashi, S. Tajik, M. Rezapour and B. Larijani, *Int. J. Electrochem. Sci.*, 2018, **13**, 2519.
72 H. Rao, M. Chen, H. Ge, Z. Lu, X. Liu, P. Zou, X. Wang, H. He, X. Zeng and Y. Wang, *Biosens. Bioelectron.*, 2017, **87**, 1029.
73 G. G. Gerent and A. Spinelli, *J. Hazard. Mater.*, 2017, **330**, 105.
74 S. Chitravathi and N. Munichandraiah, *J. Electroanal. Chem.*, 2016, **764**, 93.
75 B. Su, H. Shao, N. Li, X. Chen, Z. Cai and X. Chen, *Talanta*, 2017, **166**, 126.
76 H. Jin, C. Zhao, R. Gui, X. Gao and Z. Wang, *Anal. Chim. Acta*, 2018, **1025**, 154.
77 A. L. Suherman, K. Ngamchuea, E. E. Tanner, S. V. Sokolov, J. Holter, N. P. Young and R. G. Compton, *Anal. Chem.*, 2017, **89**, 7166.
78 M. Taei, F. Hasanpour, H. Salavati, S. H. Banitaba and F. Kazemi, *Mater. Sci. Eng., C*, 2016, **59**, 120.
79 R. Devasenathipathy, C. Karuppiah, S. M. Chen, V. Mani, V. S. Vasantha and S. Ramaraj, *Microchim. Acta*, 2015, **182**, 727.
80 R. Devasenathipathy, V. Mani, S. M. Chen, K. Kohilarani and S. Ramaraj, *Int. J. Electrochem. Sci.*, 2015, **10**, 682.
81 X. Wang, C. Luo, L. Li and H. Duan, *J. Electroanal. Chem.*, 2015, **757**, 100.
82 Z. Zheng, Q. Feng, J. Li and C. Wang, *Sens. Actuators, B*, 2015, **221**, 1162.
83 B. Kaur, R. Srivastava and B. Satpati, *RSC Adv.*, 2015, **5**, 95028.
84 L. Wu, J. Li and H. M. Zhang, *Electroanalysis*, 2015, **27**, 1195.
85 V. Mani, S. T. Huang, R. Devasenathipathy and T. C. Yang, *RSC Adv.*, 2016, **6**, 38463.
86 D. Geng, M. Li, X. Bo and L. Guo, *Sens. Actuators, B*, 2016, **237**, 581.
87 N. Shadjou, M. Hasanzadeh, F. Talebi and A. P. Marjani, *Nanocomposites*, 2016, **2**, 18.
88 Y. Wang, W. Wang, G. Li, Q. Liu, T. Wei, B. Li, C. Jiang and Y. Sun, *Microchim. Acta*, 2016, **183**, 3221.
89 M. Taei, F. Hasanpour, S. Habibollahi and L. Shahidi, *J. Electroanal. Chem.*, 2017, **789**, 140.
90 N. Amini, M. Shamsipur, M. B. Gholivand and A. Barati, *Microchem. J.*, 2017, **131**, 9.
91 M. Amiri, M. Salavati-Niasari and A. Akbari, *Microchim. Acta*, 2017, **184**, 825.
92 N. Yusoff, P. Rameshkumar and N. M. Huang, *Microchim. Acta*, 2018, **185**, 246.
93 G. Ziyatdinova, E. Kozlova and H. Budnikov, *Electrochim. Acta*, 2018, **270**, 369.
94 S. Yang, Y. Zheng, X. Zhang, S. Ding, L. Li and W. Zha, *J. Solid State Electrochem.*, 2016, **20**, 2037.
95 Y. Li, R. Liu, Q. Wang, Q. Tang, F. Liu and J. Jia, *J. Iran. Chem. Soc.*, 2019, **16**, 201.
96 C. K. Prabhu, N. Manjunatha, A. Shambhulinga, M. Imadadulla, K. H. Shivaprasad, M. K. Amshumali and K. S. Lokesh, *J. Electroanal. Chem.*, 2019, **834**, 130.
97 P. A. Rasheed, R. P. Pandey, K. A. Jabbar, J. Ponraj and K. A. Mahmoud, *Anal. Methods*, 2019, **11**, 3851.
98 K. Atacan, *J. Alloys Compd.*, 2019, **791**, 391.
99 J. Wang, *Analyst*, 1994, **119**, 763.
100 H. Beitollahi, H. Mahmoudi-Moghaddam and S. Tajik, *Anal. Lett.*, 2019, **52**, 1432.
101 F. Arduini, L. Micheli, D. Moscone, G. Palleschi, S. Piermarini, F. Ricci and G. Volpe, *TrAC, Trends Anal. Chem.*, 2016, **79**, 114.
102 M. R. Ganjali, Z. Dourandish, H. Beitollahi, S. Tajik, L. Hajiaghababaei and B. Larijani, *Int. J. Electrochem. Sci.*, 2018, **13**, 2448.
103 H. Beitollahi, F. Garkani-Nejad, S. Tajik and M. R. Ganjali, *Iran. J. Pharm. Res.*, 2019, **18**, 80.
104 S. Tajyani and A. Babaei, *J. Electroanal. Chem.*, 2018, **808**, 50.
105 A. Gevaerd, C. E. Banks, M. F. Bergamini and L. H. Marcolino-Junior, *Sens. Actuators, B*, 2020, **307**, 127547.
106 Y. Zhang, X. Jiang, J. Zhang, H. Zhang and Y. Li, *Biosens. Bioelectron.*, 2019, **130**, 315.
107 N. Jeromiyas, E. Elaiyappillai, A. S. Kumar, S. T. Huang and V. Mani, *J. Taiwan Inst. Chem. Eng.*, 2019, **95**, 466.
108 L. G. Mohtar, P. Aranda, G. A. Messina, M. A. Nazareno, S. V. Pereira, J. Raba and F. A. Bertolino, *Microchem. J.*, 2019, **144**, 13.
109 N. Hernández-Ibáñez, I. Sanjuán, M. Á. Montiel, C. W. Foster, C. E. Banks and J. Iniesta, *J. Electroanal. Chem.*, 2017, **793**, 77.
110 M. Singh, N. Jaiswal, I. Tiwari, C. W. Foster and C. E. Banks, *J. Electroanal. Chem.*, 2018, **829**, 230.
111 F. Cao, Q. Dong, C. Li, D. Kwak, Y. Huang, D. Song and Y. Lei, *Electroanalysis*, 2018, **30**, 1133.
112 A. Kurniawan, F. Kurniawan, F. Gunawan, S. H. Chou and M. J. Wang, *Electrochim. Acta*, 2019, **293**, 318.